Kidney and Blood Pressure Research

Research Article

Kidney Blood Press Res 2023;48:45–55
DOI: 10.1159/000527140

Received: October 15, 2021
Accepted: June 20, 2022
Published online: November 18, 2022

Long Noncoding RNA HOXA-AS2 Facilitates Prostate Cancer Progression by Inhibiting miR-885-5p to Upregulate KDM5B

Zhi Yang Fan Zhang Kai Cai Jianxin Xu

Department of Urology, The Sixth Hospital of Wuhan, Wuhan, China

Keywords
Long noncoding RNA · HOXA-AS2 · Prostate cancer · miR-885-5p · KDM5B

Abstract

Introduction: The regulatory network of competing endogenous RNAs (ceRNAs) affects tumorigenesis. In this study, we aimed to investigate the mechanism by which long noncoding RNA HOXA-AS2 promotes prostate cancer (PCa) progression. ***Methods:*** The expression levels of HOXA-AS2, miR-885-5p, and KDM5B in PCa tissues and cell lines were evaluated by qRT-PCR or Western blotting. CCK-8 assay, caspase-3 activity assay, flow cytometry, and scratch test revealed changes in cell proliferation, caspase-3 activity, apoptosis, and migration, respectively. Luciferase and radioimmunoprecipitation assays were used to evaluate the correlation among HOXA-AS2, miR-885-5p, and KDM5B expression profiles. ***Results:*** HOXA-AS2 expression level was elevated in PCa tissues and cells. Silencing of HOXA-AS2 suppressed proliferation and migration and facilitated apoptosis in PCa cells. HOXA-AS2 competitively adsorbed miR-885-5p, thereby blocking the effect of HOXA-AS2 knockdown by the miR-885-5p inhibitor in PCa cells. Moreover, KDM5B, a target of miR-885-5p, neutralized the function of miR-885-5p in PCa cells. ***Conclusion:*** This study revealed a potential ceRNA regulatory pathway in which HOXA-AS2 affects KDM5B expression levels by sponging miR-885-5p to promote PCa development and progression.

Introduction

Prostate carcinoma (PCa) is a leading cancer worldwide, especially in Western countries such as the USA [1]. Although the incidence of PCa in Asia is slightly lower than that in developed Western countries, it has been increasing in recent years [2]. Advances in screening techniques have increased the rate of early diagnosis of PCa [3]. However, there is still no recognized standard diagnostic method, and the study of the molecular and cellular mechanisms underlying PCa development is currently a major research focus. Unraveling the molecular mechanisms promoting PCa is crucial and may offer disease-specific therapeutic opportunities.

Long noncoding RNAs (lncRNAs) are noncoding RNAs >200 nucleotides in length [4]. Studies have shown that abnormally expressed lncRNAs promote the occurrence and development of PCa and can be used as biomarkers and therapeutic targets for the early diagnosis of PCa [5–8]. For instance, lncRNA MEG3 prevents the ma-

Karger@karger.com
www.karger.com/kbr

Correspondence to:
Jianxin Xu, jianxinxu6@163.com

lignancy of PCa in vitro [9], and enrichment of lncRNA CCAT1 in the cytoplasm facilitates the tumor growth of PCa in vivo and in vitro [10]. The lncRNA HOXA-AS2 is a regulatory factor related to tumor progression that was discovered in recent years. HOXA-AS2 is highly expressed in many carcinomas, such as colorectal cancer [11] and acute myeloid leukemia [12]. The carcinogenicity of lncRNA HOXA-AS2 is mainly mediated via inhibition or promotion of the expression of related genes through direct or indirect pathways, suggesting that HOXA-AS2 may be a viable biomarker or therapeutic target in human cancers [13]. A previous study revealed that HOXA-AS2 promotes cell migration, invasion, and epithelial-to-mesenchymal transition in PCa [14]. However, the mechanism of HOXA-AS2 in PCa is complex and requires further exploration.

MicroRNAs (miRNAs) are noncoding RNAs that inhibit protein expression through base pairing, thus affecting the process of mRNA translation or degradation [15]. The effects of miR-885-5p vary in different cancers. For example, miR-885-5p promotes malignancy in gastric cancer [16] but suppresses progression in osteosarcoma [17]. However, the detailed effect of miR-885-5p in PCa has not been elucidated. As noncoding lncRNAs and protein-coding mRNAs have miRNA response elements that can bind miRNAs, they compete for limited miRNAs and form a competitive endogenous RNA (ceRNA) regulatory network [18]. miR-885-5p has been found to regulate this regulatory mechanism in cancer. Gao et al. [19] revealed that HSP90AA1-IT1 shares the same binding site with CDK2, a key regulator of glioma formation, and competitively binds to miR-885-5p. In addition, a previous study showed that HOXA-AS2 acts as a ceRNA to regulate miR-885-5p expression, thereby regulating glioblastoma carcinogenesis [20]. However, the mechanism by which HOXA-AS2 regulates miR-885-5p to mediate PCa remains unknown.

KDM5B is a Jumonji C domain-containing histone demethylase belonging to the KDM5 family that is closely related to tumor progression [21]. KDM5B is upregulated in multiple cancers, such as breast cancer [22], gastric cancer [16], and ovarian cancer [23]. KDM5B is overexpressed in PCa, and KDM5B knockdown significantly suppresses the malignancy of PCa cells [24, 25]. However, the upstream mechanism through which KDM5B contributes to PCa remains unclear.

Based on the results of previous studies, we hypothesized that the HOXA-AS2/miR-885-5p/KDM5B axis may participate in PCa progression via a ceRNA mechanism. Our findings may provide novel insights into PCa progression.

Materials and Methods

Collection of Tissue Samples and Cell Culture

PCa and adjacent non-tumor tissues were collected from 34 patients diagnosed with PCa at our hospital between May 2016 and September 2018. The baseline clinical characteristics of the patients are listed in online supplementary Table 1 (for all online suppl. material, see www.karger.com/doi/10.1159/000527140). This study was approved by the Ethics Committee of our hospital and sought informed consent from the patients.

All cell lines were obtained from the American Type Culture Collection (ATCC, USA). A human prostatic epithelial cell line (RWPE1) was cultured in keratinocyte serum-free medium (Invitrogen, USA) containing EGF (Invitrogen) and bovine pituitary extract (Invitrogen), whereas the PCa cell lines (22RV1, DU145, and LNCaP) were cultured in Dulbecco's modified Eagle's medium (Thermo Fisher Scientific, USA) containing 10% fetal bovine serum (Thermo Fisher Scientific) and 1% penicillin/streptomycin (Thermo Fisher Scientific). All the cells were incubated at 37°C with 5% CO_2.

Cell Transfection

siRNA plasmids used to silence HOXA-AS2/KDM5B (si-HOXA-AS2/si-KDM5B), negative control siRNA (si-NC), HOXA-AS2 overexpression (OE-HOXA-AS2), OE-NC, miR-885-5p mimic/inhibitor, mimic-NC, and inhibitor-NC were obtained from GenePharma (Shanghai, China). Using Lipofectamine® 2000 (Thermo Fisher Scientific), 22RV1 and DU145 cells (~70% confluent) were transfected with 50 nM si-HOXA-AS2 or si-KDM5B, 2 μg/mL OE-HOXA-AS2, 50 nM miR-885-5p mimic or inhibitor, and corresponding negative control plasmids including 50 nM si-NC, 50 nM mimic-NC, and 50 nM inhibitor-NC or 2 μg/mL OE-NC at 37°C and 5% CO_2. After 48 h, qRT-PCR was performed to confirm the transfection efficiency.

qRT-PCR

Total RNA was extracted using TRIzol® (Invitrogen, USA) reagent. After extraction, the RNA was reverse transcribed using a GoldScript One-Step RT-PCR Kit (Applied Biosystems Inc., USA), and qRT-PCR was performed using a SYBR® Premix Ex Taq II PCR Kit (TaKaRa, China). Primer sequences are shown in Table 1. The relative expression was analyzed using the $2^{-\Delta\Delta Ct}$ method using U6 as the internal reference for miR-885-5p and GAPDH as the internal reference for HOXA-AS2 and KDM5B.

Nuclear-Cytoplasmic Fractionation

Nuclear-cytoplasmic fractionation was performed using an Ambion PARIS™ kit (Invitrogen). The cells were lysed by incubating them with lysis buffer on ice for 10 min. The lysates were collected and centrifuged at 3,000 *g* for 10 min. The supernatant constituted the cytoplasm, and the precipitate mainly contained the nucleus. RNA was extracted from the cytoplasm and nucleus in an ice bath followed by qRT-PCR.

Western Blot Analysis

Total protein was extracted from the cells using radioimmunoprecipitation assay (RIPA) buffer (Beyotime, China), and the protein concentration was determined using a BCA protein concentration detection kit (Beyotime, China). Then, 30 μg of proteins were separated by 10% sodium dodecyl sulfate polyacrylamide gel

Table 1. PCR primer sequences

Gene	Forward	Reverse
HOXA-AS2	CCCGTAGGAAGAACCGATGA	TTTAGGCCTTCGCAGACAGC
miR-885-5p	GTCCATTACACTACCCTGCCTC	CGCGAGCACAGAATTAATACG
miR-3174	GTCAGGGATGGCAACTTTATCCACT	GGAACCTGAAGGTCCGAGTCA
miR-2116-3p	AATCCTATGCCAAGAACTCCC	CTCTACAGCTATATTGCCAGCCA
KDM5B	ATTGCCTCAAAGGAATTTGGCAGTG	CATCACTGGCATGTTGTTCAAATTC
U6	CTCGCTTCGGCAGCACA	AACGCTTCACGAATTTGCGT
GAPDH	GCAAATTCCATGGCACCGTC	TCGCCCCACTTGATTTTGG

electrophoresis, transferred to polyvinylidene difluoride membranes, and blocked with 5% skim milk. Next, the membranes were incubated with primary antibodies against KDM5B (1:1,000, Abcam, USA) and GAPDH (1:1,000, Abcam, USA) at 4°C for 12 h. After incubation with the primary antibodies, the membranes were incubated with an HRP-conjugated secondary antibody (1:5,000, Abcam, USA) for 3 h at 37°C. The protein bands in the membranes were visualized using an ECL reagent (Sigma-Aldrich, USA).

Cell Counting Kit-8 (CCK-8) Assay

Cells (5×10^3 cells/well) were plated in a 96-well plate. After culturing, 10 μL/well of CCK-8 reagent (Sigma, USA) was added to the cells every 24 h and incubated for 4 h. The absorbance was measured at 450 nm using a microplate reader.

Caspase-3 Activity Assay

Two million cells were collected and lysed with 100 μL lysis buffer on ice for 15 min. After centrifuging at 4°C for 10 min at 15,000 × *g*, the supernatant was used to detect caspase-3 activity using the Caspase-3 Activity Assay Kit (Beyotime Biotechnology Inc., China) according to the manufacturer's instructions. After incubating at 37°C for 2 h, the optical density of each sample was determined at 405 nm using a microplate reader.

Flow Cytometric Assay

Cell apoptosis was evaluated using an Annexin V/FITC Apoptosis Detection Kit (BD Biosciences, USA) according to the manufacturer's recommendations. Briefly, the cells were harvested, washed twice with cold phosphate-buffered saline, and resuspended in 1× binding buffer. Then, the cells were stained with 5 μL annexin V-FITC and PI for 15 min by incubating at room temperature in the dark. The stained cells were analyzed using a FACSCalibur flow cytometer (BD Biosciences) with the Cell Quest Pro software, and the percentage of apoptotic cells was calculated.

Scratch Assay

After transfection, the PCa cells were seeded in 6-well plates and cultured until 90% confluent. Then, a 100-μL tip was used to create scratches in the cell monolayer. After washing off the detached cells with phosphate-buffered saline, the adherent cells were incubated in medium without fetal bovine serum for 24 h. Images of the scratches were captured at 0 and 24 h using an inverted microscope.

Luciferase Assay

The binding sites on HOXA-AS2 and KDM5B 3′-UTR were inserted into the psiCHECK2 vector (Promega, USA) to construct wild-type (WT) HOXA-AS2 and KDM5B. The binding sites on HOXA-AS2 and KDM5B 3′-UTR were mutated and inserted into the psiCHECK2 vector to construct mutant-type (MUT) HOXA-AS2/KDM5B. The WT or MUT HOXA-AS2/KDM5B plasmids were transfected into 22RV1 and DU145 cells along with mimic-NC or miR-885-5p mimic. Subsequently, luciferase assays were performed using the Dual Luciferase Reporter Gene Assay Kit (Beyotime, China). The luciferase activity was measured on a Promega Glomax™ 20/20 luminescence detector.

RIP Assay

The assay was performed using an RIP kit (Millipore, USA). After lysing the cells with RIP lysis buffer, RIP buffer containing magnetic beads (Invitrogen) conjugated to anti-Ago2 or anti-IgG (negative control) antibody was added to the lysates. Subsequently, the samples were treated with proteinase K, and the immunoprecipitated RNA was detected using qRT-PCR.

Statistical Analysis

All assays were conducted in triplicate, and the data are presented as the mean ± standard deviation. Statistical significance was compared between the two groups using Student's *t* test (two tailed), whereas one-way ANOVA was used to analyze the statistical significance among multiple groups using GraphPad Prism 7.0 (GraphPad, USA). Statistical significance was set at $p < 0.05$.

Results

HOXA-AS2 Knockdown Abates the Malignancy of PCa Cells

HOXA-AS2 expression profiles in PCa and RWPE1 cells (normal control) revealed that the PCa cells (22RV1, DU145, and LNCaP) expressed higher levels of HOXA-AS2 compared to RWPE1 cells (Fig. 1a). In addition, compared to the adjacent normal tissues, HOXA-AS2 expression level was elevated in PCa tissues (Fig. 1b). Next, we explored the relationship between HOXA-AS2 expression and clinicopathological charac-

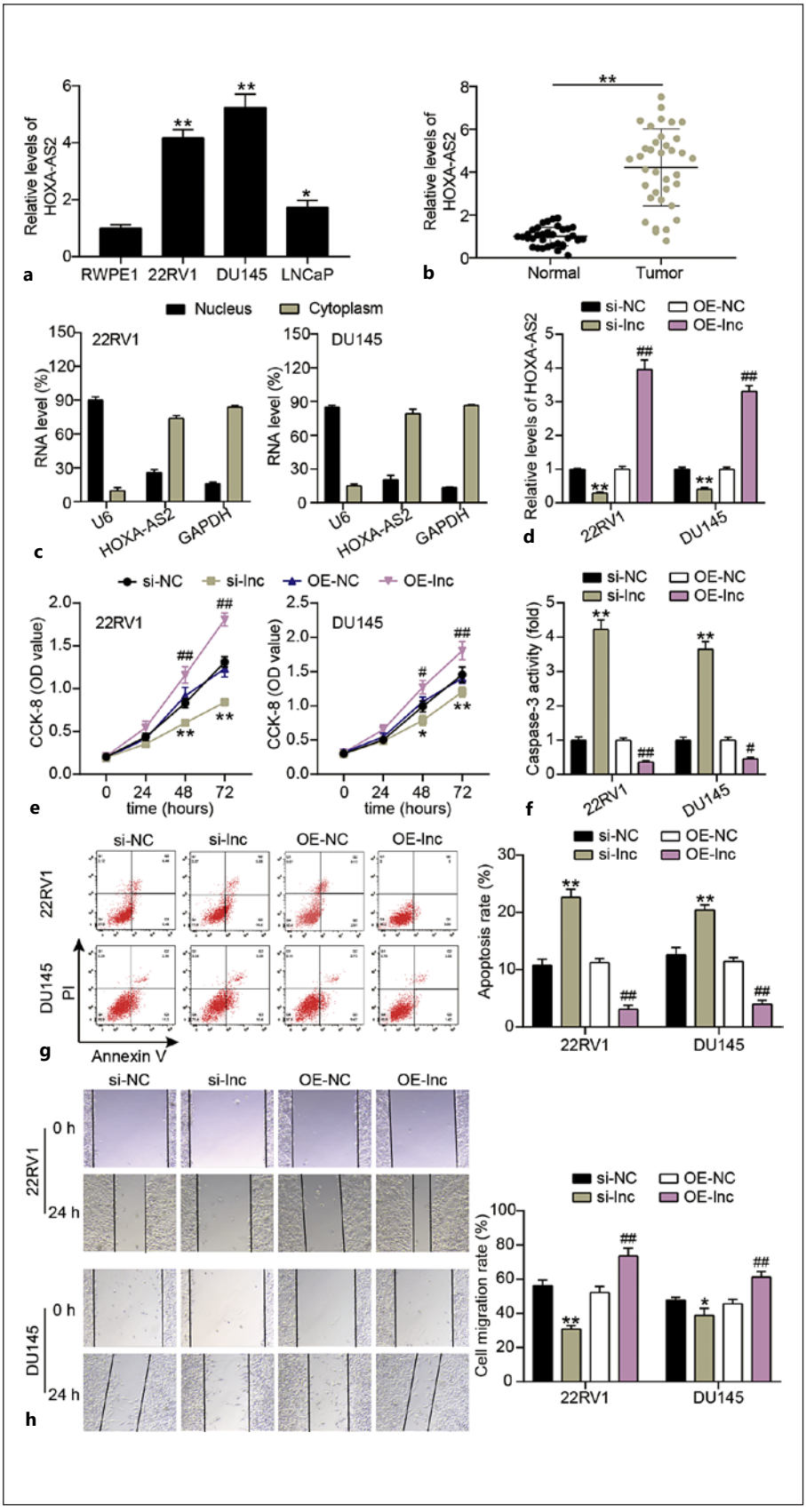

Fig. 1. Effect of silencing HOXA-AS2 on PCa cells. **a** The expression level of HOXA-AS2 was measured by qRT-PCR in the RWPE1 and PCa cells (22RV1, DU145, and LNCaP). $^{**}p < 0.001$ versus RWPE1 cells. **b** The expression level of HOXA-AS2 was measured by qRT-PCR in the PCa tissues ($N = 34$) and adjacent normal tissues ($N = 34$). $^{**}p < 0.001$. **c** The location of HOXA-AS2 in 22RV1 and DU145 cells was measured via nuclear-cytoplasmic fractionation. **d** The expression level HOXA-AS2 was measured by qRT-PCR in 22RV1 and DU145 cell lines transfected with si-lnc and OE-lnc. **e** Cell proliferation was measured via CCK-8 assay in 22RV1 and DU145 cells transfected with si-lnc and OE-lnc. **f** Caspase-3 activity was measured via caspase-3 activity assay in 22RV1 and DU145 cells transfected with si-lnc and OE-lnc. **g** Apoptosis was measured via flow cytometry assay in 22RV1 and DU145 cells transfected with si-lnc and OE-lnc. **h** Cell migration rate was measured via scratch test assay in 22RV1 and DU145 cells transfected with si-lnc and OE-lnc. si-lnc, si-HOXA-AS2; NC, negative control; OE-lnc, OE-HOXA-AS2. $N = 3$, data are presented as mean ± SD, $^{**}p < 0.001$ versus si-NC; $^{\#\#}p < 0.001$ versus OE-NC.

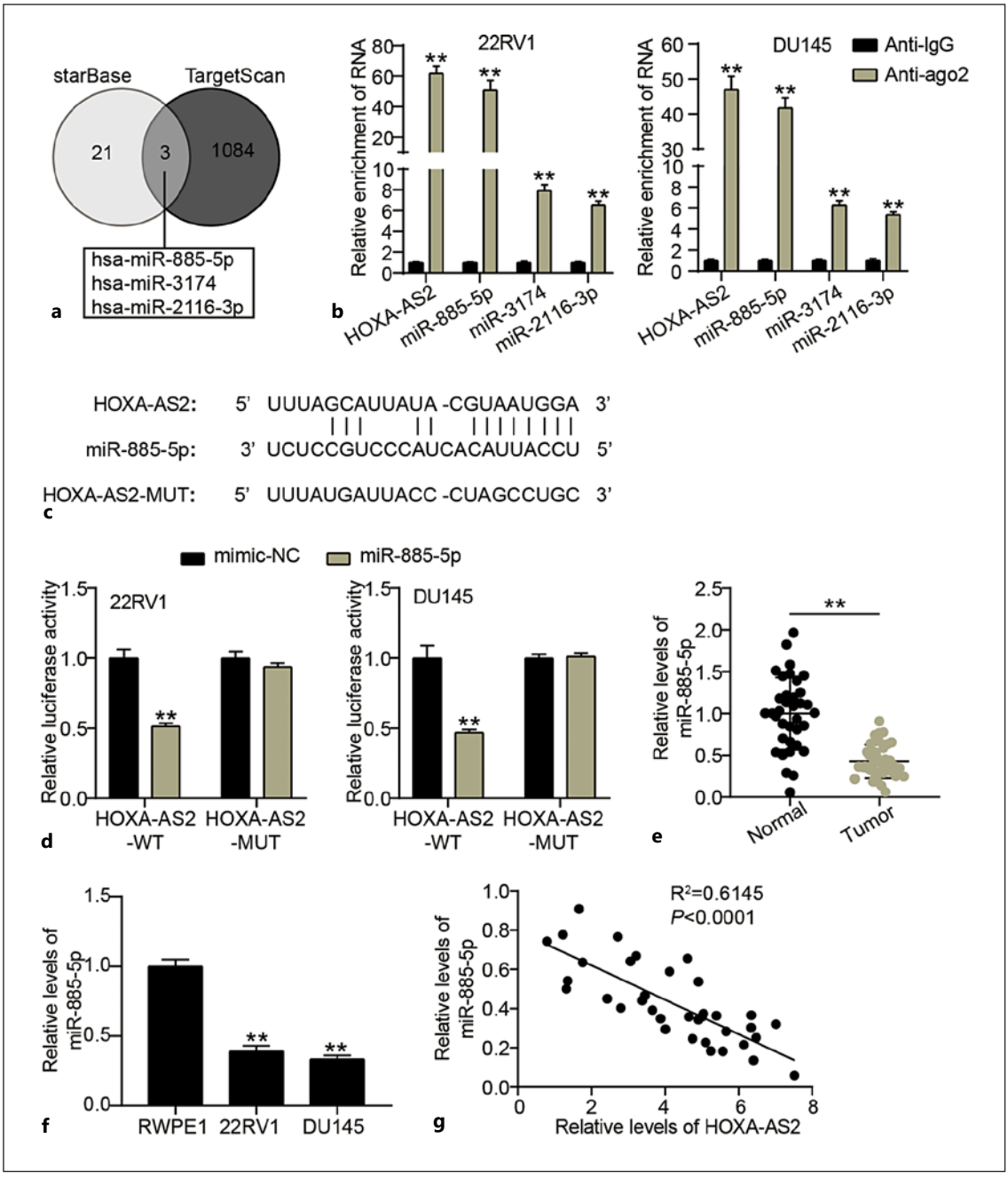

Fig. 2. miR-885-5p was sponged by HOXA-AS2. **a** Three miRNAs were overlapped from starBase and TargetScan. starBase and TargetScan were used to predict the miRNAs binding to HOXA-AS2 and KDM5B, respectively. **b** RNA RIP assay was performed in 22RV1 and DU145 cells followed by qRT-PCR. $^{**}p < 0.001$ versus IgG. **c** The binding sites between miR-885-5p and HOXA-AS2 were predicted via starBase. **d** The luciferase activity in cells transfected with miR-885-5p and WT or MUT HOXA-AS2 was detected via luciferase assay. WT, wild type; MUT, mutant type. $^{**}p < 0.001$ versus mimic-NC. **e** The expression level of miR-885-5p was measured by qRT-PCR in RWPE and PCa cells (22RV1, DU145, and LNCaP). $^{**}p < 0.001$. **f** The expression level of miR-885-5p was measured by qRT-PCR in the PCa tissues ($N = 34$) and adjacent normal tissues ($N = 34$). $^{**}p < 0.001$ versus RWPE1 cells. **g** The correlation analysis of miR-885-5p and HOXA-AS2 was evaluated via Pearson analysis. $N = 3$, data are presented as mean ± SD.

teristics of PCa patients. We divided all the cases into HOXA-AS2 high- and low-expression groups (n = 17 each). As summarized in online Supplementary Table 1, HOXA-AS2 high expression level was strongly associated with advanced clinical T stage, lymph node involvement, distant metastasis, and a high Gleason score. However, HOXA-AS2 expression was not associated with age or the specimen type. Next, we evaluated the subcellular localization of HOXA-AS2 and found that HOXA-AS2 was mainly located in the cytoplasm (Fig. 1c). Following transfection of 22RV1 and DU145 cells with si-HOXA-AS2, HOXA-AS2 expression level decreased by approximately 60%. Transfection of 22RV1 and DU145 cells with OE-HOXA-AS2 resulted in approximately 3.5-fold increase in HOXA-AS2 expression level (Fig. 1d). Cell proliferation and caspase-3 activity were analyzed in these cells using CCK-8 and caspase-3 activity assays, respectively. The results showed that si-HOXA-AS2 suppressed the proliferative ability and resulted in apoptosis of PCa cells, whereas OE-HOXA-AS2 had the opposite effect (Fig. 1e–f). In addition, flow cytometric analysis showed that the apoptotic rate of PCa cells increased in the si-HOXA-AS2 group and decreased in the OE-HOXA-AS2 group compared to that in the corresponding control group (Fig. 1g; see online suppl data files). Furthermore, the scratch assay results revealed that the rate of cell migration decreased following HOXA-AS2 downregulation and increased upon HOXA-AS2 upregulation (Fig. 1h; see online suppl data files).

MiR-885-5p Is Sponged by HOXA-AS2

Based on starBase analysis, high expression level of KDM5B correlated with poor prognosis in PCa (online suppl. Fig. 1); therefore, we identified KDM5B as a gene of interest. Then, starBase was used to predict the miRNAs that bind to HOXA-AS2, and TargetScan was used to predict the miRNAs that target KDM5B. The starBase and TargetScan results showed that miR-885-5p, miR-3174, and miR-2116-3p were common miRNAs (Fig. 2a). We then performed RIP assay and found that the enrichment of HOXA-AS2 and miR-885-5p was increased in the Ago2 group (Fig. 2b), suggesting a correlation between them. The binding sites on HOXA-AS2 were predicted using starBase (Fig. 2c). Luciferase assay verified that the luciferase activity in the HOXA-AS2-WT + miR-885-5p group was lower than that in the HOXA-AS2-WT + miR-NC group; however, the luciferase activity in the HOXA-AS2-MUT + miR-885-5p group showed no distinct change (Fig. 2d). qRT-PCR results showed that miR-885-5p expression level was lower in PCa cells (22RV1 and DU145) than that in RWPE1 cells (Fig. 2e). Moreover, we also found that miR-885-5p expression level was lower in PCa tissues and was negatively correlated with HOXA-AS2 expression level (Fig. 2f–g).

miR-885-5p Knockdown Reverses the Effect of si-HOXA-AS2

Next, to examine the role of miR-885-5p in the biological characteristics of PCa cells, si-HOXA-AS2 and miR-885-5p inhibitors were transfected into cells. miR-885-5p expression level decreased in cells transfected with the miR-885-5p inhibitor but was elevated in cells following HOXA-AS2 knockdown (Fig. 3a). The results of the CCK-8 assay showed that cell proliferation in the miR-885-5p inhibitor group was enhanced, and downregulation of miR-885-5p reversed the negative effect of HOXA-AS2 knockdown on cell proliferation (Fig. 3b). Caspase-3 activity assay revealed that caspase-3 activity was suppressed following transfection with the miR-885-5p inhibitor, but caspase-3 activity in cells co-transfected with miR-885-5p inhibitor and si-HOXA-AS2 was similar to that in si-NC or inhibitor-NC (Fig. 3c). Similarly, flow cytometry showed that miR-885-5p knockdown reduced the apoptotic rate and partially abolished the pro-apoptotic effect of HOXA-AS2 knockdown (Fig. 3d; see online suppl data files). The scratch assay revealed that the migration ability of cells was clearly elevated following transfection with the miR-885-5p inhibitor, and inhibition of miR-885-5p reversed the negative effect of HOXA-AS2 knockdown on cell migration (Fig. 3e; see online suppl data files).

Fig. 3. miR-885-5p inhibitor reversed the effect of silencing HOXA-AS2. **a** The expression level of miR-885-5p was measured by qRT-PCR in 22RV1 and DU145 cells transfected with si-lnc and inhibitor. **b** Cell proliferation was measured via CCK-8 assay in 22RV1 and DU145 cells transfected with si-lnc and inhibitor. **c** Caspase-3 activity was measured via caspase-3 activity assay in 22RV1 and DU145 cells transfected with si-lnc and inhibitor. **d** Apoptosis was measured via flow cytometry assay in 22RV1 and DU145 cells transfected with si-lnc and inhibitor. **e** Cell migration rate was measured via scratch test assay in 22RV1 and DU145 cells transfected with si-lnc and inhibitor. si-lnc, si-HOXA-AS2; NC, negative control; inhibitor, miR-885-5p inhibitor. N = 3, data are presented as mean ± SD, $^{**}p < 0.001$ versus si-NC; $^{\&\&}p < 0.001$ versus inhibitor; $^{\#\#}p < 0.001$ versus si-lnc + inhibitor.

(For figure see next page.)

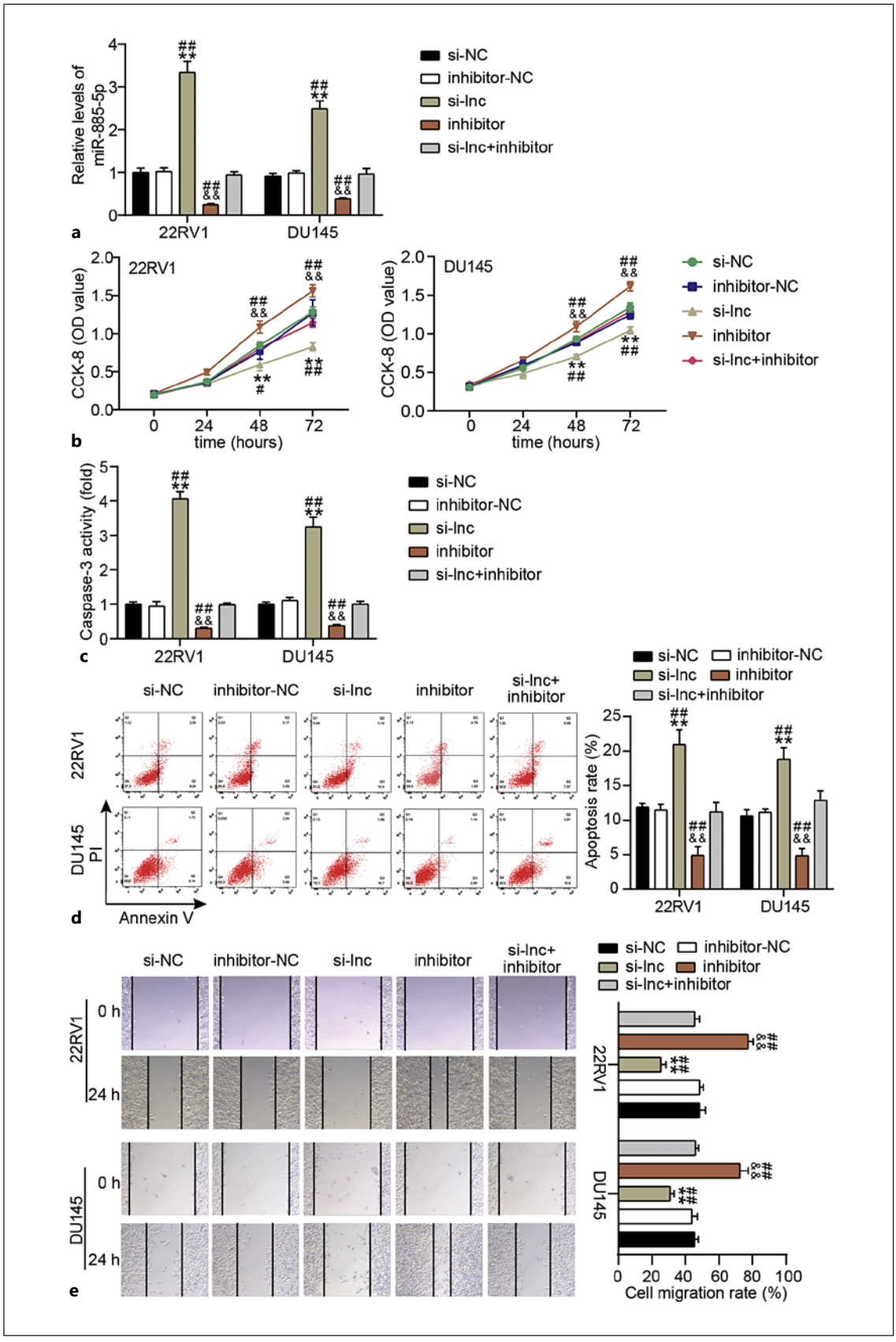

3

MiR-885-5p Targets KDM5B

The binding sites of miR-885-5p in the 3′-UTR of KDM5B predicted by TargetScan are shown in Figure 4a. Luciferase assay revealed that the relative luciferase activity was reduced following co-transfection of cells with KDM5B-WT and miR-885-5p, whereas co-transfection with KDM5B-MUT and miR-885-5p did not affect the relative luciferase activity (Fig. 4b). qRT-PCR assay showed that KDM5B expression level was higher in PCa tissues and cells compared to that in adjacent normal tissues and RWPE1 cells (Fig. 4c–d). Moreover, KDM5B expression in PCa tissues was negatively correlated with miR-885-5p expression (Fig. 4e).

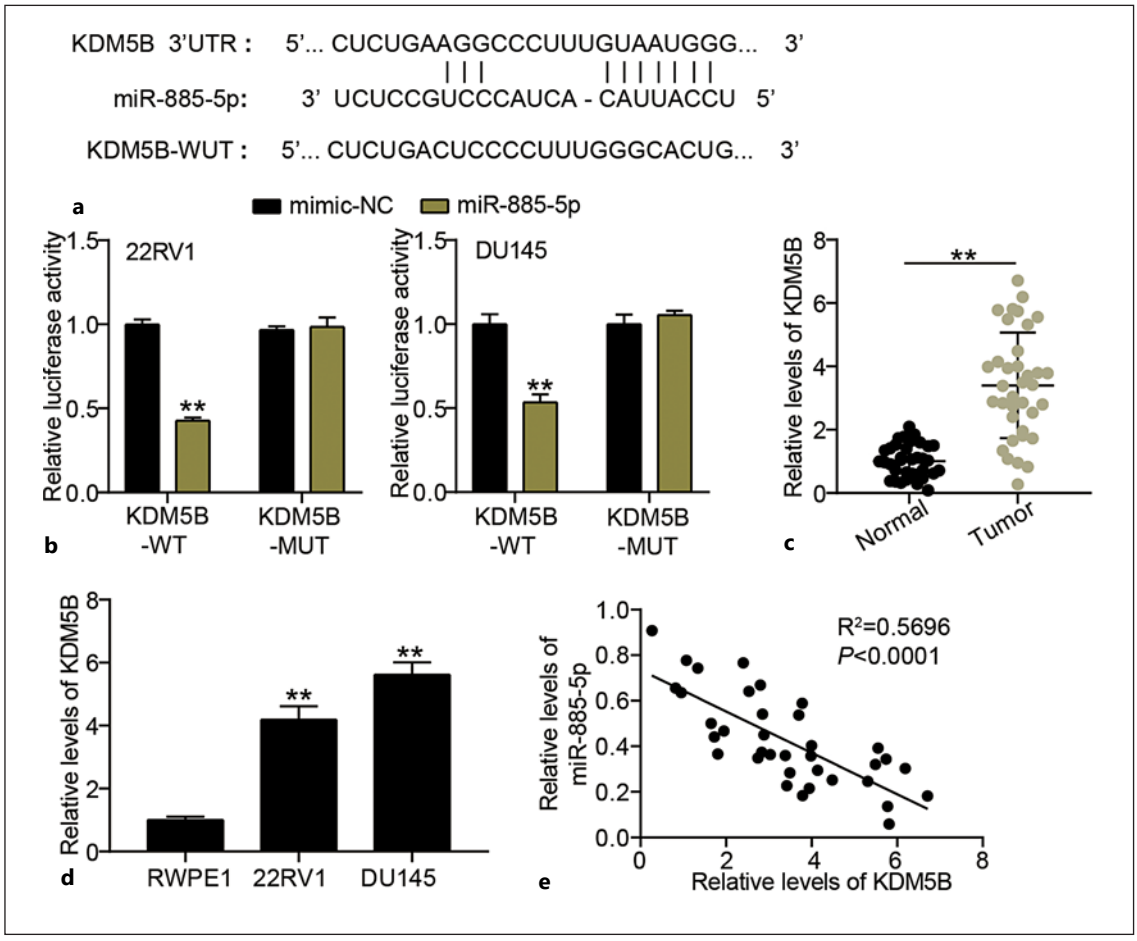

Fig. 4. MiR-885-5p targets KDM5B. **a** The binding sites between miR-885-5p and KDM5B predicted by TargetScan. **b** The luciferase activity in cells transfected with miR-885-5p and WT or MUT KDM5B was detected by luciferase assay. WT, wild type; MUT, mutant type. $^{**}p < 0.001$ versus mimic-NC. **c** The expression level of HOXA-AS2 was measured by qRT-PCR in the PCa tissues ($N = 34$) and adjacent normal tissues. $^{**}p < 0.001$. **d** The expression level of KDM5B was measured by qRT-PCR in RWPE and PCa cells (22RV1, DU145, and LNCaP). $^{**}p < 0.001$ versus RWPE1 cells. **e** The correlation analysis of miR-885-5p and KDM5B was evaluated via Pearson analysis. $N = 3$, data are presented as mean ± SD.

Fig. 5. si-KDM5B reversed the effect of miR-885-5p inhibitor on PCa cells. **a** The expression level KDM5B was measured by Western blot in transfected 22RV1 and DU145 cells transfected with si-KDM5B and inhibitor. **b** Cell proliferation was measured via CCK-8 assay in 22RV1 and DU145 cells transfected with si-KDM5B and inhibitor. **c** Caspase-3 activity was measured via caspase-3 activity assay in 22RV1 and DU145 cells transfected with si-KDM5B and inhibitor. **d** Apoptosis was measured via flow cytometry assay in 22RV1 and DU145 cells transfected with si-KDM5B and inhibitor. **e** Cell migration rate was measured via scratch test assay in 22RV1 and DU145 cells transfected with si-KDM5B and inhibitor. NC, negative control; inhibitor, miR-885-5p inhibitor. $N = 3$, data are presented as mean ± SD, $^{**}p < 0.001$ versus si-NC; $^{\&\&}p < 0.001$ versus inhibitor; $^{\#\#}p < 0.001$ versus si-KDM5B + inhibitor.

(For figure see next page.)

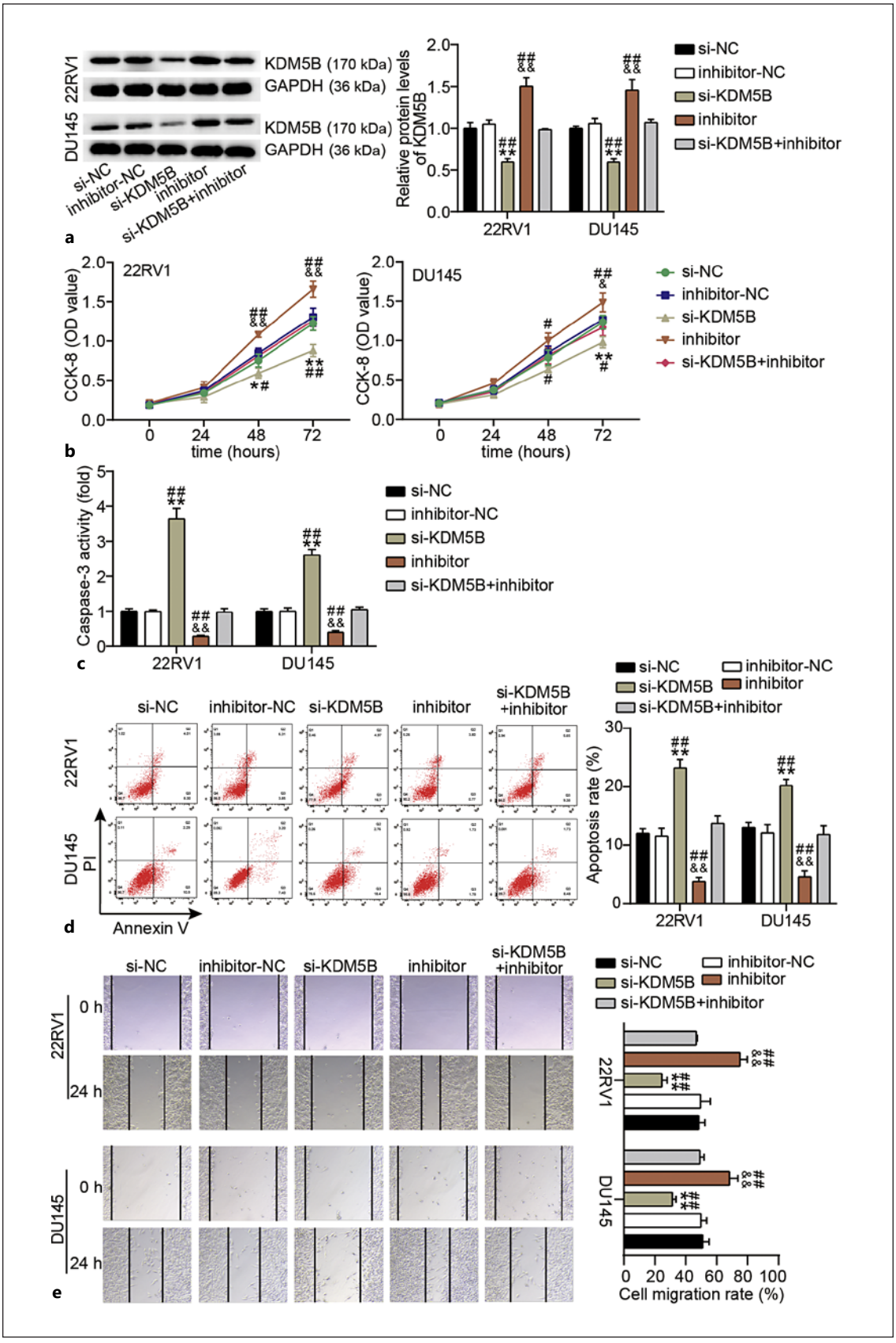

5

miR-885-5p Inhibits PCa Progression by Mediating the Expression of KDM5B

To confirm the function of miR-885-5p and KDM5B in PCa, si-KDM5B and miR-885-5p inhibitors were used to silence KDM5B and miR-885-5p, respectively. Western blot analysis indicated that si-KDM5B decreased the expression level of KDM5B protein, whereas the miR-885-5p inhibitor had the opposite effect (Fig. 5a; see online suppl data files). Furthermore, si-KDM5B impaired cell proliferation; however, this effect was reversed by the miR-885-5p inhibitor (Fig. 5b). Caspase-3 activity assay revealed that caspase-3 activity was increased by si-KDM5B, whereas miR-885-5p inhibitor reversed the positive effect of si-KDM5B (Fig. 5c). Flow cytometry revealed an increase in the apoptotic rate in the si-KDM5B group, whereas the miR-885-5p inhibitor reversed the si-KDM5B-mediated promotion of apoptosis (Fig. 5d; see online suppl data files). The results of the scratch assay showed that the rate of cell migration declined in the si-KDM5B group, and the miR-885-5p inhibitor reversed the decrease in migration rate caused by si-KDM5B (Fig. 5e; see online suppl data files).

Discussion

PCa is a major type of cancer worldwide owing to the lack of standard diagnostic methods. Our investigation found upregulation of HOXA-AS2 and KDM5B along with a downregulation of miR-885-5p in PCa. Furthermore, our study demonstrated that the downregulation of HOXA-AS2 reduced the proliferation and migration of PCa cells and increased apoptosis in PCa cells. We determined that the effect of silencing HOXA-AS2 on PCa cells was reversed by an miR-885-5p inhibitor because of their targeting relationship. In addition, miR-885-5p inhibited PCa progression by mediating the expression of KDM5B. In conclusion, HOXA-AS2 promotes PCa progression by targeting miR-885-5p to upregulate KDM5B.

HOXA-AS2 plays a pro-oncogenic role in various cancers. For example, a study revealed that HOXA-AS2 expression level is elevated in hepatoblastoma and promotes malignant biological behaviors in hepatoblastoma [26]. Another study reported that HOXA-AS2 functions as an oncogene in acute myeloid leukemia in vitro and in vivo [27]. In the current study, HOXA-AS2 was upregulated in PCa tissues and cells, and silencing of HOXA-AS2 decreased the proliferation and migration of PCa cells – this finding was consistent with previous studies. Consistent with our results, a previous study showed that HOXA-AS2 was elevated in PCa, and silencing HOXA-AS2 inhibited the malignancy of PCa cells [14]. Additionally, a study reported that HOXA-AS2-mediated sponging of miR-885-5p inhibited glioblastoma development [20]. This is consistent with our study showing that HOXA-AS2 serves as a ceRNA of miR-885-5p, thereby directly reducing miR-885-5p expression level. In our study, we observed a downregulation of miR-885-5p in PCa tissues and cells, and the negative role of HOXA-AS2 knockdown in PCa cells was reversed by miR-885-5p knockdown.

miR-885-5p acts as a tumor suppressor in multiple cancers such as hepatocellular carcinoma [28] and osteosarcoma [17]. However, the role of miR-885-5p in PCa has not been explored. Here, we fill the knowledge gap in this field by showing that miR-885-5p knockdown promotes cell proliferation and migration in PCa cells, suggesting that miR-885-5p is a tumor suppressor in PCa also. We also showed that KDM5B is a target of miR-885-5p, and its effect on PCa is regulated by miR-885-5p.

Another interesting finding of this study is that miR-885-5p inhibited the progression of PCa by mediating the expression of KDM5B. A recent study reported that KDM5B governs PI3K/AKT signaling in PCa, and KDM5B knockdown significantly decreases the proliferation of PCa cells [29]. Regarding the role of KDM5B in cell migration, a previous study showed that KDM5B knockdown inhibited PCa cell migration [25]. These results are consistent with our findings that KDM5B knockdown suppresses the malignant phenotypes in PCa.

Although our study demonstrates that HOXA-AS2 regulates the miR-885-5p/KDM5B axis and promotes PCa progression, it has some limitations. The results of this study need to be further verified by increasing the sample size and the number of animal experiments in the future. Carcinogenesis involves complex signaling pathways, and the downstream mechanisms of the effect of KDM5B remain to be studied and validated. In conclusion, our study suggests that inhibition of HOXA-AS2 may prevent PCa malignancy. These findings may facilitate novel therapeutic strategies for treating PCa.

Statement of Ethics

The present study was approved by the Ethics Committee of the Sixth Hospital of Wuhan (approval No. WSHKY2016-019). The processing of clinical tissue samples is in strict compliance with the ethical standards of the Declaration of Helsinki. All patients signed written informed consent. The study complies with the ISSCR Guidelines for the Conduct of Human Embryonic Stem Cell Research. All participants signed written informed consent.

Conflict of Interest Statement

The authors declare that there is no conflict of interest.

Author Contributions

Zhi Yang designed the study. Fan Zhang performed most of the experiments. Kai Cai and Jianxin Xu collected the data and wrote the paper. All authors read and approved the final manuscript.

Funding Sources

This work was supported by Municipal Health Commission General Project "The role and mechanism of histone demethylase KDM5B in prostate cancer" (WX19D17).

Data Availability Statement

All data and original images generated or analyzed during this study are included in this article or supplementary material. Further inquiries can be directed to the corresponding author.

References

1 Yang T, Jing Y, Dong J, Yu X, Zhong M, Pascal LE, et al. Regulation of ELL2 stability and polyubiquitination by EAF2 in prostate cancer cells. Prostate. 2018 Nov;78(15):1201–12.
2 Yan W, Li H, Zhou Y, Huang Z, Rong S, Xia M, et al. Prostate carcinoma spatial distribution patterns in Chinese men investigated with systematic transperineal ultrasound guided 11-region biopsy. Urol Oncol. 2009 Sep–Oct;27(5):520–4.
3 Tomlins SA, Day JR, Lonigro RJ, Hovelson DH, Siddiqui J, Kunju LP, et al. Urine TMPRSS2:ERG plus PCA3 for individualized prostate cancer risk assessment. Eur Urol. 2016 Jul;70(1):45–53.
4 Jandura A, Krause HM. The new RNA world: growing evidence for long noncoding RNA functionality. Trends Genet. 2017 Oct;33(10):665–76.
5 Zhang H, Meng H, Huang X, Tong W, Liang X, Li J, et al. lncRNA MIR4435-2HG promotes cancer cell migration and invasion in prostate carcinoma by upregulating TGF-β1. Oncol Lett. 2019 Oct;18(4):4016–21.
6 Ge S, Mi Y, Zhao X, Hu Q, Guo Y, Zhong F, et al. Characterization and validation of long noncoding RNAs as new candidates in prostate cancer. Cancer Cell Int. 2020 Nov 1;20(1):531.
7 De Summa S, Palazzo A, Caputo M, Iacobazzi RM, Pilato B, Porcelli L, et al. Long non-coding RNA landscape in prostate cancer molecular subtypes: a feature selection approach. Int J Mol Sci. 2021 Feb 23;22(4):2227.
8 Zhao H, Dong H, Wang P, Zhu H. Long noncoding RNA SNHG17 enhances the aggressiveness of C4-2 human prostate cancer cells in association with β-catenin signaling. Oncol Lett. 2021 Jun;21(6):472.
9 Wu M, Huang Y, Chen T, Wang W, Yang S, Ye Z, et al. LncRNA MEG3 inhibits the progression of prostate cancer by modulating miR-9-5p/QKI-5 axis. J Cell Mol Med. 2019 Jan;23(1):29–38.
10 You Z, Liu C, Wang C, Ling Z, Wang Y, Wang Y, et al. LncRNA CCAT1 promotes prostate cancer cell proliferation by interacting with DDX5 and MIR-28-5P. Mol Cancer Ther. 2019 Dec;18(12):2469–79.
11 Ding J, Xie M, Lian Y, Zhu Y, Peng P, Wang J, et al. Long noncoding RNA HOXA-AS2 represses P21 and KLF2 expression transcription by binding with EZH2, LSD1 in colorectal cancer. Oncogenesis. 2017 Jan 23;6(1):e288.
12 Huang R, Liao X, Wang X, Li Q. Comprehensive investigation of the clinical significance of long non-coding RNA HOXA-AS2 in acute myeloid leukemia using genome-wide RNA sequencing dataset. J Cancer. 2021;12(7):2151–64.
13 Wang J, Su Z, Lu S, Fu W, Liu Z, Jiang X, et al. LncRNA HOXA-AS2 and its molecular mechanisms in human cancer. Clin Chim Acta. 2018 Oct;485:229–33.
14 Xiao S, Song B. LncRNA HOXA-AS2 promotes the progression of prostate cancer via targeting miR-509-3p/PBX3 axis. Biosci Rep. 2020 Aug 28;40(8):BSR20193287.
15 Bartel DP. MicroRNAs: target recognition and regulatory functions. Cell. 2009 Jan 23;136(2):215–33.
16 Li S, Sun MY, Su X. MiR-885-5p promotes gastric cancer proliferation and invasion through regulating YPEL1. Eur Rev Med Pharmacol Sci. 2019 Sep;23(18):7913–9.
17 Liu Y, Bao Z, Tian W, Huang G. miR-885-5p suppresses osteosarcoma proliferation, migration and invasion through regulation of β-catenin. Oncol Lett. 2019 Feb;17(2):1996–2004.
18 Zhou RS, Zhang EX, Sun QF, Ye ZJ, Liu JW, Zhou DH, et al. Integrated analysis of lncRNA-miRNA-mRNA ceRNA network in squamous cell carcinoma of tongue. BMC Cancer. 2019 Aug 7;19(1):779.
19 Gao T, Gu G, Tian J, Zhang R, Zheng X, Wang Y, et al. LncRNA HSP90AA1-IT1 promotes gliomas by targeting miR-885-5p-CDK2 pathway. Oncotarget. 2017 Sep 26;8(43):75284–97.
20 Shou J, Gao H, Cheng S, Wang B, Guan H. LncRNA HOXA-AS2 promotes glioblastoma carcinogenesis by targeting miR-885-5p/RBBP4 axis. Cancer Cell Int. 2021 Jan 11;21(1):39.
21 Yang Z, Qiu Q, Chen W, Jia B, Chen X, Hu H, et al. Structure of the arabidopsis JMJ14-H3K4me3 complex provides insight into the substrate specificity of KDM5 subfamily histone demethylases. Plant Cell. 2018 Jan;30(1):167–77.
22 Wang J, Chen L, Zhang Y, Li CG, Zhang H, Wang Q, et al. Association between serum vitamin B(6) concentration and risk of osteoporosis in the middle-aged and older people in China: a cross-sectional study. BMJ Open. 2019 Jul 4;9(7):e028129.
23 Ren R, Wu J, Zhou MY. MiR-135b-5p affected malignant behaviors of ovarian cancer cells by targeting KDM5B. Eur Rev Med Pharmacol Sci. 2020 Nov;24(22):11469.
24 Xiang Y, Zhu Z, Han G, Ye X, Xu B, Peng Z, et al. JARID1B is a histone H3 lysine 4 demethylase up-regulated in prostate cancer. Proc Natl Acad Sci U S A. 2007 Dec 4;104(49):19226–31.
25 Yang Z, Xu JX, Fang DP, Ke J. Analysis of key genes reveal lysine demethylase 5B promotes prostate cancer progression. Oncol Lett. 2020 Oct;20(4):62.
26 Liu G, Liu B, Liu X, Xie L, He J, Zhang J, et al. ARID1B/SUB1-activated lncRNA HOXA-AS2 drives the malignant behaviour of hepatoblastoma through regulation of HOXA3. J Cell Mol Med. 2021 Apr;25(7):3524–36.
27 Feng Y, Hu S, Li L, Peng X, Chen F. Long noncoding RNA HOXA-AS2 functions as an oncogene by binding to EZH2 and suppressing LATS2 in acute myeloid leukemia (AML). Cell Death Dis. 2020 Dec 2;11(12):1025.
28 Jin Y, Zhang M, Duan R, Yang J, Yang Y, Wang J, et al. Long noncoding RNA FGF14-AS2 inhibits breast cancer metastasis by regulating the miR-370-3p/FGF14 axis. Cell Death Discov. 2020 Oct 12;6(1):103.
29 Chen Y, Gao H, Li Y. Inhibition of LncRNA FOXD3-AS1 suppresses the aggressive biological behaviors of thyroid cancer via elevating miR-296-5p and inactivating TGF-β1/Smads signaling pathway. Mol Cell Endocrinol. 2020 Jan 15;500:110634.